Award # 04HQGR004

LATEST PLEISTOCENE PALEOSEISMOLOGY OF THE SOUTHERN LITTLE SALMON FAULT, STRONG'S CREEK, FORTUNA, CALIFORNIA

FINAL TECHNICAL REPORT

Mark A. Hemphill-Haley
Department of Geology
One Harpst Streeet
Humboldt State University
Arcata, CA 95521
707-826-3933 (phone)
707-826-5241 (fax)
markhh@humboldt.edu

Robert C. Witter
Oregon Department of Geology and Mineral Industries
Coastal Field Office
313 SW 2nd St., Suite D.
Newport, OR 97365
541-574-7969 (phone)
541- 265-5241 (fax)
rob_witter@dogami.state.or.us

TABLE OF CONTENTS

LIST OF FIGURES

LIST OF TABLES

LATEST PLEISTOCENE PALEOSEISMOLOGY OF THE SOUTHERN LITTLE SALMON FAULT, STRONG'S CREEK, FORTUNA, CALIFORNIA

Mark A. Hemphill-Haley, Robert C. Witter and Humboldt Friends of Geology (F.O.G.)

ABSTRACT

A trench was excavated along a southern splay of the Little Salmon fault near Fortuna, California. The Little Salmon fault is one of the southernmost reverse faults within the onland fold and thrust belt associated with the Cascadia subduction zone. The trench exposed evidence for at least 3 fold and fault events in terrace gravels and overbank deposits associated with nearby Strong's Creek. A prominent 1 m-wide fault zone dipping between 30 and 60° displaces all but the uppermost unit in the trench which is anthropogenic fill. The majority of deformation appears related to non-brittle folding of the fine-grained deposits. The most recent event consisted of about 2.5 m of vertical uplift and 2.9 m of horizontal shortening in a broad monoclinal fold of a prominent clayey silt deposit accompanied by about 20 cm of reverse offset. This event occurred between about 10,000 to 12,000 years ago. Based on retrodeformation of trench units and radiocarbon-based estimates of deposit ages, we conclude that a total of 5.1 m of fault parallel offset has occurred since about 13,000 to 14,000 years ago providing a slip rate of about 0.4 to 0.5 mm/yr. The three deformation events occurred within a span of less than 4,000 years followed by 10,000 years of quiescence. We conclude that this may represent temporal clustering of events on this particular splay of the fault which is not characteristic of the Little Salmon fault as a whole. Ample evidence for multiple Holocene ruptures on the Little Salmon fault at locations to the north lead us to believe that the splay trenched at Strong's Creek is likely subsidiary to a more active, yet unmapped structure nearby.

[1] Department of Geology, One Harpst St. Humboldt State University, Arcata, CA 95521 Phone (707) 826-3933; E-mail: markhh@humboldt.edu

[2]Oregon Department of Geology and Mineral Industries Coastal Field Office, 313 SW 2nd St., Suite D., Newport, OR 97365 Phone (541) 574-7969; Fax: (541) 265-5241 E-mail: rob_witter@dogami.state.or.us

ACKNOWLEDGEMENTS

This project would never have been possible without the amazing volunteer work of numerous people. We would like to thank them all personally but there is a limit to the size of the paper. Pacific Lumber Co. was extremely gracious to this study. Not only did they give us permission to excavate the trench but they also provided an excavator and operator at no charge. We'd like to thank John Oswald and his staff at PALCO for all of their logistical and geological help. The Humboldt Friends of Geology (F.O.G.) is an informal group of earth scientists that meets every two months to talk about geology and geology-related topics. A large number of members of the group provided countless hours to the task of cleaning, shoring, flagging, gridding, logging and photographing the trench, thank you. Of this group, several local area consulting firms provided staff to help in the project, the include SHN Engineers and Geologists, Pacific Watershed Associates, LACO Associates, Stillwater Sciences. We would specifically like to thank

Dr. Tom Stephens of SHN Engineers for showing us the Little Salmon fault exposed in a nearby road cut, especially since he had not seen it for many years. Thomas Dunklin photographed the south wall of the trench and provided valuable insight into how to collect digital trench images. We were also assisted by faculty at Humboldt State University, especially Dr. Harvey Kelsey and Dr. Sue Cashman. Many students from the Department of Geology at HSU provided mental- and labor-intensive hours to the project. I would like to specifically thank Andy Tate and Emily Fudge who conducted specific projects under the guidance of Dr. Sue Cashman at the trench. We were also assisted by geologists from Humboldt County This project was generously funded by the U.S. Geological Survey National Earthquake Hazards Reduction Program Grant #04HQPA0001.

INTRODUCTION

The Little Salmon fault (LSF) is one of the southernmost faults within the Little Salmon fault zone (LSfz), a major contractional structure located at the southern end of the Cascadia onland fold and thrust belt (Carver and Burke, 1992). The onland fold and thrust belt represents the upper plate deformation front associated with the Cascadia subduction zone (CSZ) (Figure 1).

Objectives of this investigation included: 1) better constraint of the timing and size of upper-plate earthquakes along the Little Salmon fault and 2) establish a deformation chronology on an inland portion of the fault away from the influences of marsh-related geology that might be attributable to coseismic coastal subsidence.

One complexity regarding the history of rupture along the LSF is its association with the CSZ. Does the LSF act as an independent seismogenic structure or is it somehow structurally linked to the subduction zone megathrust (Clarke and Carver, 1992; Witter et al., 2002). One consequence of direct association between the two structures might be that the LSF ruptures in tandem with the megathrust. Conversely, if the LSF is not tied structurally to the megathrust it may then have a rupture history independent of the subduction zone.

Detailed Holocene surface rupture and coseismic subsidence chronologies have been developed at locations along the northern portion of the fault on land (for example Woodward-Clyde Consultants (1980), Carver and Burke (1988), Witter et al. (2002) and Patton (2004)) (Figure 2). Several of these investigations have compared deformation events known Cascadia megathrust coseismic events (for example Nelson et al. (1995), Atwater and Hemphill-Haley (1997) and Goldfinger et al. (2003)) to assess whether there is one-for-one correlation between the sources. However, within the influence of tidal marshes and potential tsunami-related deposits, it is difficult to separate the evidence for an LSF-induced rupture versus deformation attributable to the subduction zone.

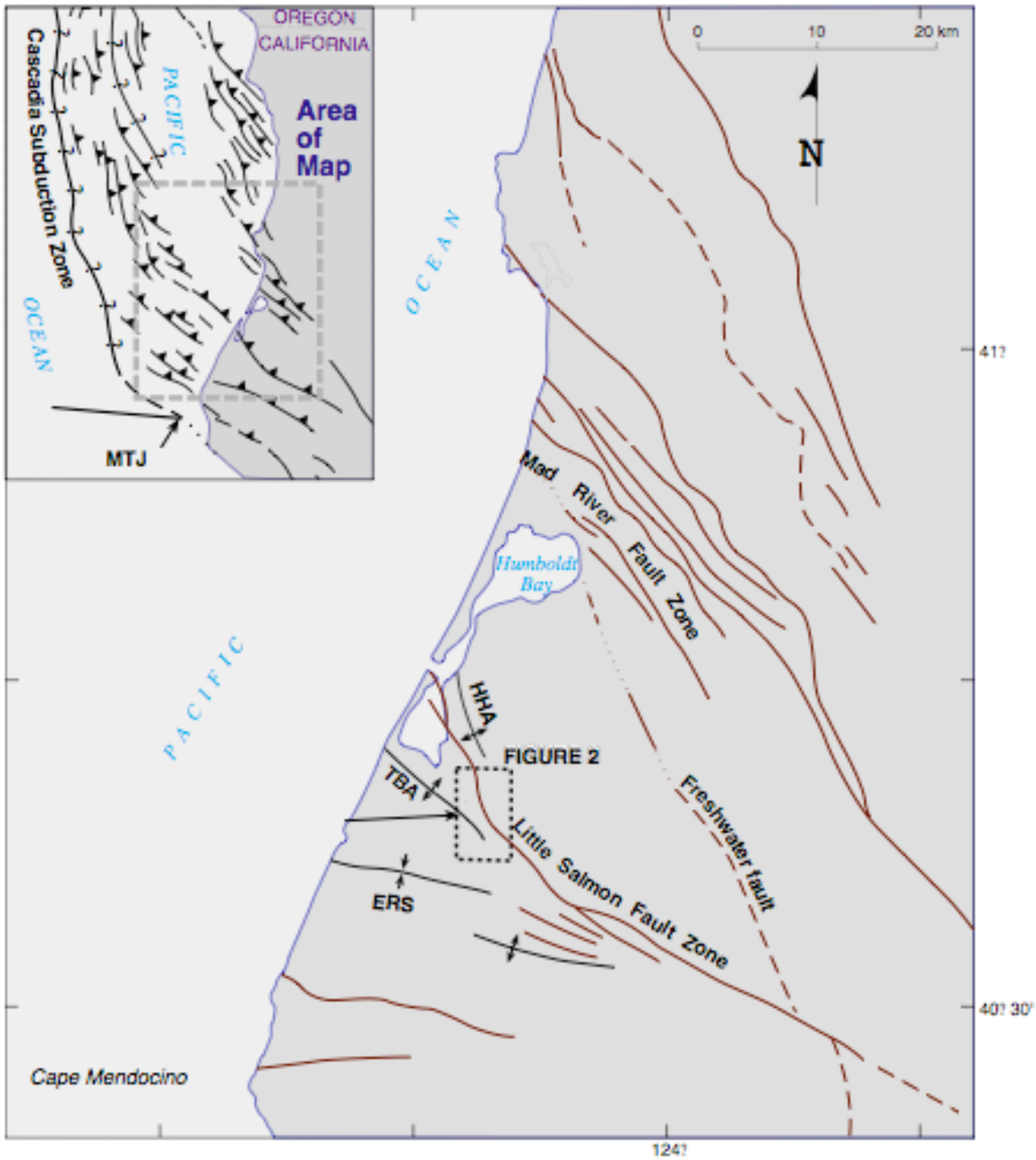

Figure 1 - Tectonic map of coastal California north of Cape Mendocino in context of the plate tectonic setting (inset). Crustal contraction in the lower Eel River valley occurs along the Little Salmon fault zone and along imbricate thrust faults of the Mad River fault zone north of Humboldt Bay. The Little Salmon fault study is shown in Figure 2. HHA, Humboldt Hill anticline; TBA, Table Bluff anticline; ERS, Eel River syncline; MTJ, Mendocino Triple Junction (From Witter et al., 2002).

One recent study by Witter et al. (2002) provides evidence of a likely event on the Little Salmon fault, at their Swiss Hall site, that occurred approximately 1,000 years ago and does not coincide with a known CSZ event.

APPROACH

This project consisted of a simple, fault normal excavation across a splay of the Little Salmon fault. We chose a location to the south of the main body of previous investigations (Figure 2) in order to collect surface rupture data for the fault away from the marsh environment and to characterize the lateral paleoseismic history of the fault.

The study area is located in Strong's Creek drainage, in the area of the former town site of Newberg directly northeast of Fortuna (Figure 2). We chose this location on the basis of previous mapping of the LSF near the range front alluvium contact (Tom Stephens, 2004, personal communication). Additionally, for much of its southern extent the fault is located in hilly terrain that is largely occupied by large landslides. The Strong's Creek site afforded us with a location absent of apparent landslide features.

The fault is exposed in a road cut along a private logging road along the north side of the drainage (Figure 3a). Based on the along strike projection of the fault, apparent fault related geomorphology of the drainage and mapping to the south of Strong's Creek by Stephens and by Kelsey (1980) we initially sited our trench across an inactive log deck (Figure 3a). We had prior information that, previously, a large lumber mill occupied the entire site (Figure 3b). Our intention was to trench through the deck fill and into the fault scarp that was buried below. However, a former timber company employee informed us that the logging deck contained large amounts of steel, including a railroad flatbed car, so we decided to abandon the primary trench site. Instead, we excavated a small, < 2 m high, broad, west-facing scarp immediately to the west of the logging deck (Figure 3a and 3c).

We excavated a single 24 m long, 4.5 m deep, 1.2 m wide, trench along a portion of the Little Salmon fault within the floodplain of Strong's Creek at an elevation of about 50 m (Figure 3c). The surface of the site is clearly disturbed by activities of the former mill site (Figure 3b) so we did not focus on geomorphic analysis of the site. This activity also impacted the upper portion of the trench stratigraphy that appears to be truncated and then backfilled.

Once we cleaned and gridded the trench walls we flagged stratigraphic contacts, structures and potential radiocarbon sample sites. We photographed, in sequence, each side of the trench in 1- by 1-m increments using a digital camera and wide-angle lens. We rectified each photo frame to remove distortion and combined the images to produce a photo record and logging base for the trench (Figure 4). We printed the mosaic for each side of the trenched and logged details using a Mylar overlay.

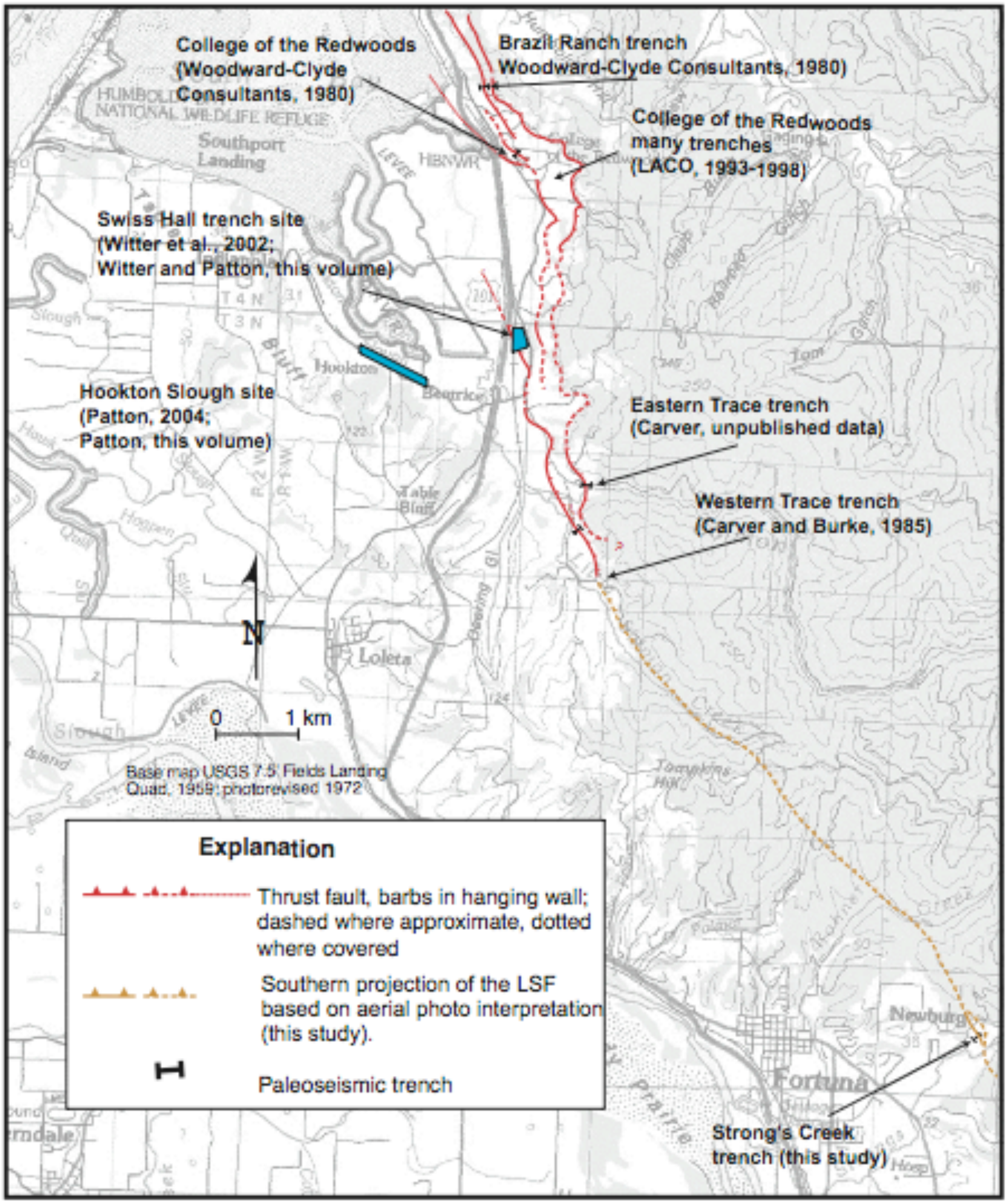

Figure 2 – Location map of a portion of the Little Salmon fault. Locations of earlier paleoseismic (Woodward-Clyde Consultants, 1980; Witter et al., 2002; Witter and Patton, this volume; Carver, unpublished and Carver and Burke, 1985), marsh stratigraphic (Patton, 2004; Patton, this volume), and fault location (Laco, this volume) studies are shown. Location of the fault south of the Carver and Burke (1985) study is uncertain and depicted here based on aerial photographic interpretation.

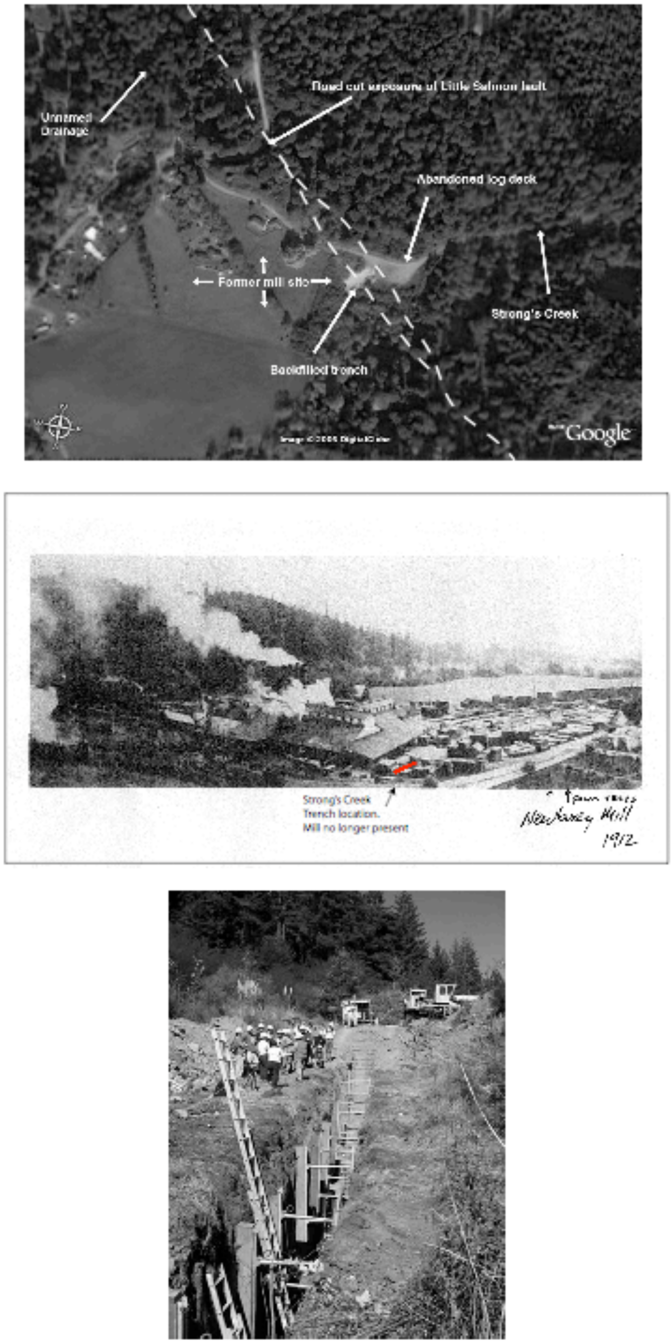

Figure 3 – Strong's Creek trench location photographs. a) aerial photograph taken from *Google Earth* map application. The backfilled trench is included in this photo. In addition, the locations of roadcut exposure of the Little Salmon fault originally mapped by Tom Stephens (SHN Engineering), Strong's Creek drainage, an unnamed drainage to the north of the site and the abandoned logging deck are shown. b) 1912 photograph of the Newberg mill. The location of the Strong's Creek trench is shown in the lower center of the photograph. The mill is no longer present, however, substantial evidence for mill-related surface disturbance still exists, c) photograph of the Strong's Creek trench taken while the trench is being visited by a Humboldt State University soils science class. Camera is pointed to the northeast. Note the broad, gentle warp toward the log deck used to park abandoned yarders).

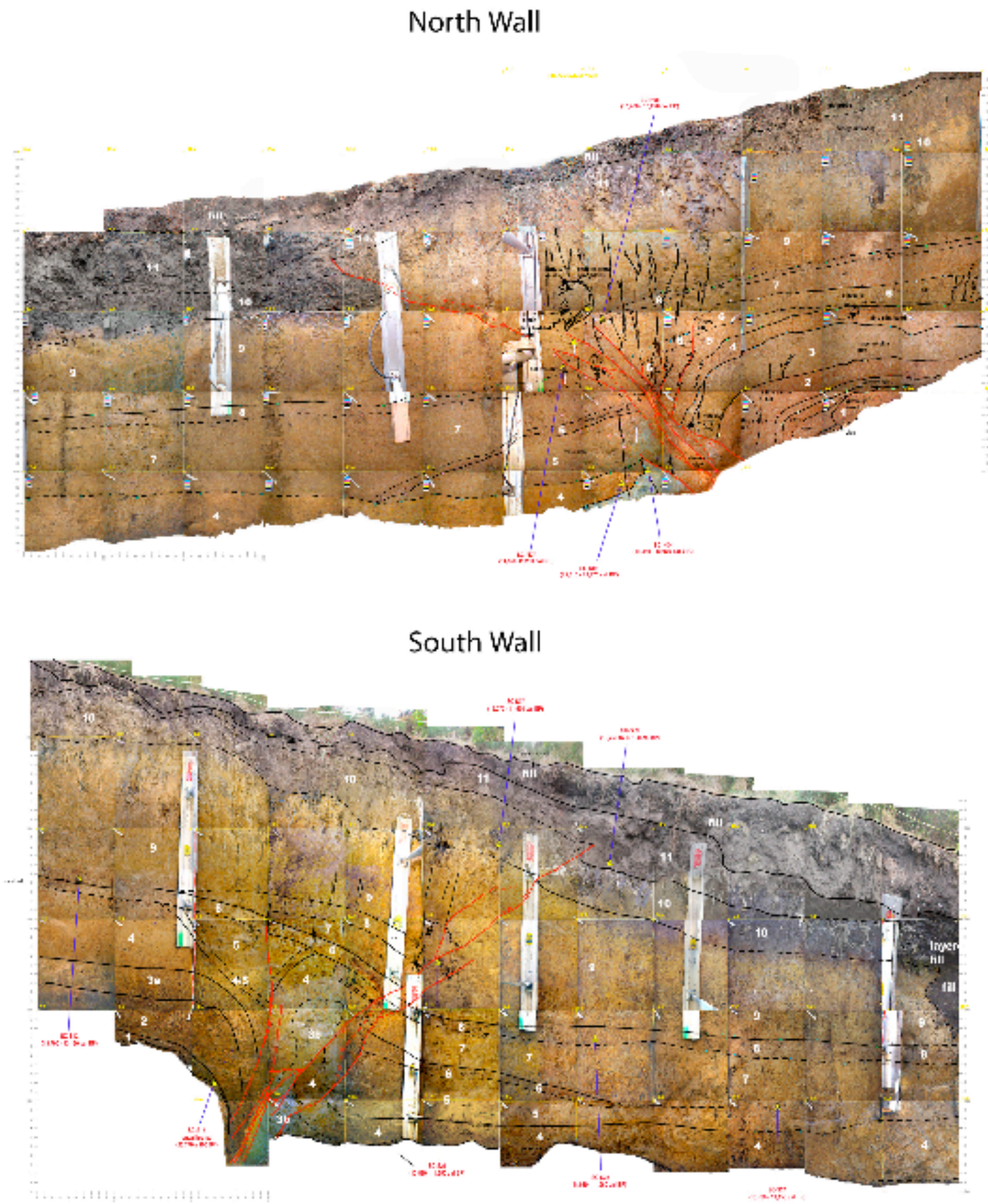

Figure 4 – Photo mosaics of the north (top) and south (bottom) walls of the Strong's Creek trench. East is to the right in the top image and to the left in the bottom image. Line drawings of principle contacts and structures are shown in addition to locations of radiocarbon sample sites. Upper portion of trench represents anthropogenic disturbance likely related to mill activities. Individual photos represent a 1 x 1 m portion of the trench.

RESULTS

The trench exposes a deep section of fine-grained sediments that we interpret to be overbank deposits related to Strong's Creek. This thick section of fine sand and silt overlies a medium to coarse-grained sand and sandy gravel deposit exposed in the base of the eastern side of the trench (Figures, 4, 5 and 6, Unit 1). A low-angle zone of shearing and associated folding truncates the basal gravel layer and deforms overlying fine-grained deposits (Figure 4). The shear zone is approximately 1 m wide but is associated with a zone of folding that extends for more than 6 m (Tate et al., 2005). The average dip of the fault is about 45NE with the E side up relative to deposits on the W (Figure 4, 5 and 6). Based on detailed structural and stratigraphic analysis of the fault and folded sediments, Tate et al. (2005) conclude that motion along the fault is almost entirely reverse dip-slip with associated drag folds in both the hanging wall and footwall.

We interpret the stratigraphic units exposed by the trench to be a sequence of rapidly deposited flood overbank deposits. They are likely related to hydraulic backfilling associated with the confluence of Strong's Creek located immediately south of the trench site and a nearby, unnamed drainage that enters the valley to the north (Figure 3a). Within the trench, a repeated sequence of clayey silty units overly sandy and silty units (Figure 5 and 6, Units 4, 6, 8, and 10). We interpret these sequences to represent either weak soils formed on the flood deposits or upward fining sequences in the overbank depositional environment. A thick anthropogenic fill deposit truncates stratigraphy across the upper part of the trench (Figure 5 and 6, Unit 12). Units are laterally truncated but traceable across the shear zone.

Detrital charcoal is plentiful throughout the trench. Eleven samples were submitted for accelerator mass spectrometer (AMS) analysis (Table 1). These radiocarbon dates allow us to estimate the ages for the faulted and folded stratigraphic section. They also provide us with a means to estimate the age of deformation events.

The basal gravel layer (Unit 1) is approximately 23,770 ± 200 yr BP (uncalibrated) while the uppermost layer that is not anthropogenic (Unit 11) has an age of 10,250 to 10,190 cal BP (Table 1, Figures 5 and 6). Charcoal within the clayey deposit at the top of the sediments directly overlying the basal gravel provides an age of approximately 13,000 to 14,000 cal BP (Table 1). Thus, there is an unconformity above the gravel unit that represents about 10,000 years of missing time. The remainder of the trench section spans about 2,500 to 3,000 years of sedimentation. Possible explanations for the origin of the unconformity above the basal gravels are purely speculative but may include a) a period of lateral planation and abandonment by Strong's Creek, tectonic uplift of the sequence by a splay of the fault to the east of the trench, or creek incision in response to sea level change.

RETRODEFORMATION

Although the zone of faulting was clearly represented in the trench, it was evident that much of the deformation was related to folding. In order to estimate the amount of folding per event, we performed a per-event retrodeformation of the trench sediments

Table 1. Radiocarbon Data for the Strong's Creek Trench, Humboldt County, California

Trench Sample No.	Laboratory Sample No.	Sample Material	Stratigraphic Unit	$\delta^{13}C$ (‰)	Lab-reported age (^{14}C yr BP at 1σ)b	Calibrated age (yr BP at 2σ)c\
Trench North Wall						
SC-N04-101404	Beta - 203041	charred material		-26.7	11230 +/- 40	13020 - 13410
SC-N05-101404	Beta - 201457	charred material		-27.3	11540 +/- 60	13170 - 13810
SC-N07-101404	Beta - 203042	charred material		-29.3	9960 +/- 40	11230 - 11550
SC-N08-101404	Beta - 203043	charred material		-26.5	9230 +/- 40	10250 - 10520
Trench South Wall						
SC-S12-100504	Beta - 203044	charred material		-28.9	11420 +/- 50	13160 - 13790
SC-S16-100504	Beta - 203045	charred material		-24.5	23770 +/- 200	-
SC-S22-100504	Beta - 203046	charred material		-25.5	10020 +/- 50	11260 - 11930
SC-S23-100504	Beta-203047	charred material		-26.7	10420 +/- 60	11950 - 12830
SC-S27-100504	Beta - 203048	charred material		-24.5	11400 +/- 50	13150 - 13680
SC-S37-101404	Beta - 203049	charred material		-24.1	10140 +/- 40	11570 - 10320
SC-S39-101504	Beta - 205933	charred material		-23.7	9080 +/- 40	10190 - 10250

a) Reported ages are corrected for \δ13C and include a laboratory error multiplier of 1.0 in reported laboratory uncertainty; samples analyzed by Beta Analytic, Inc. (radiocarbon years before present; "present"=1950AD) b) Read -25 as value of 25% measured for 13C/12C ratio; NA = not available.c) Calibrated using Stuiver and Reimer (1998).

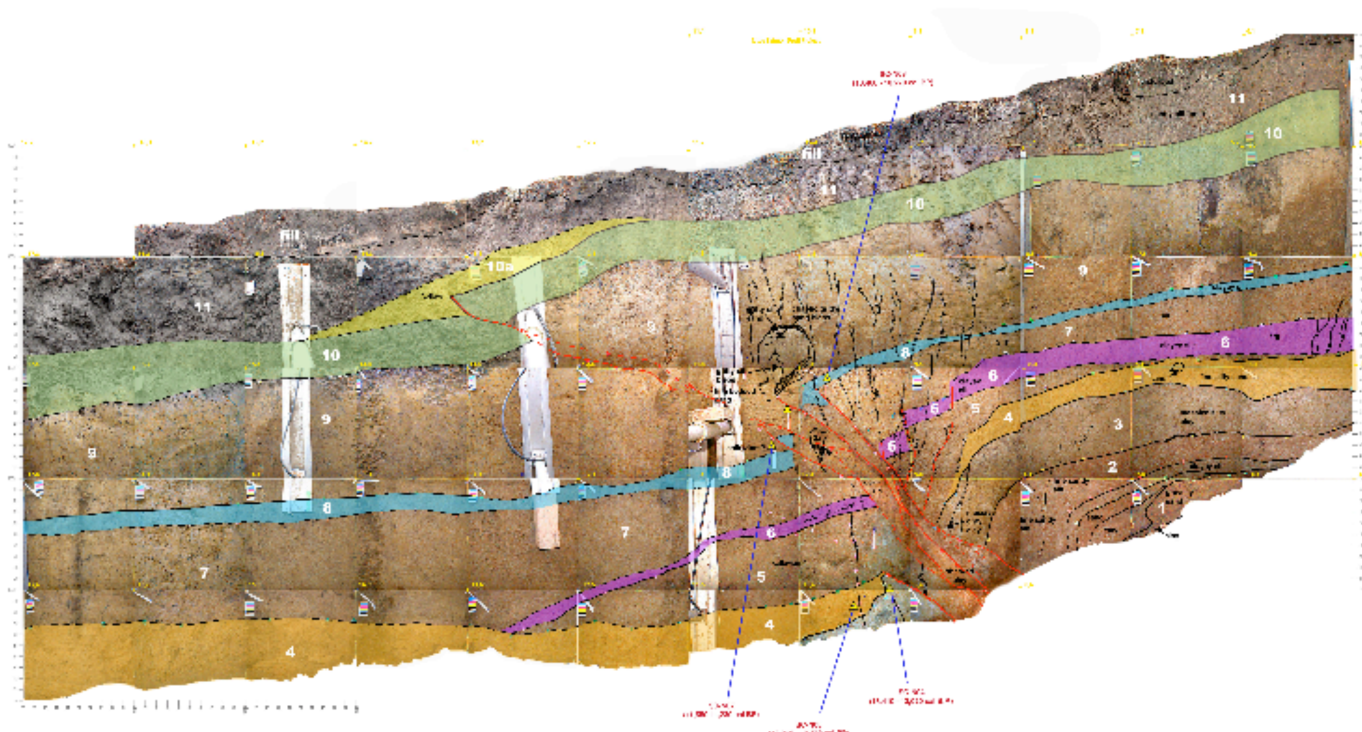

Figure 5 – Photo mosaic and interpretation of the north wall of the Strong's Creek trench. Highlighted areas represented clayey silt units that are used in the retrodeformation exercise.

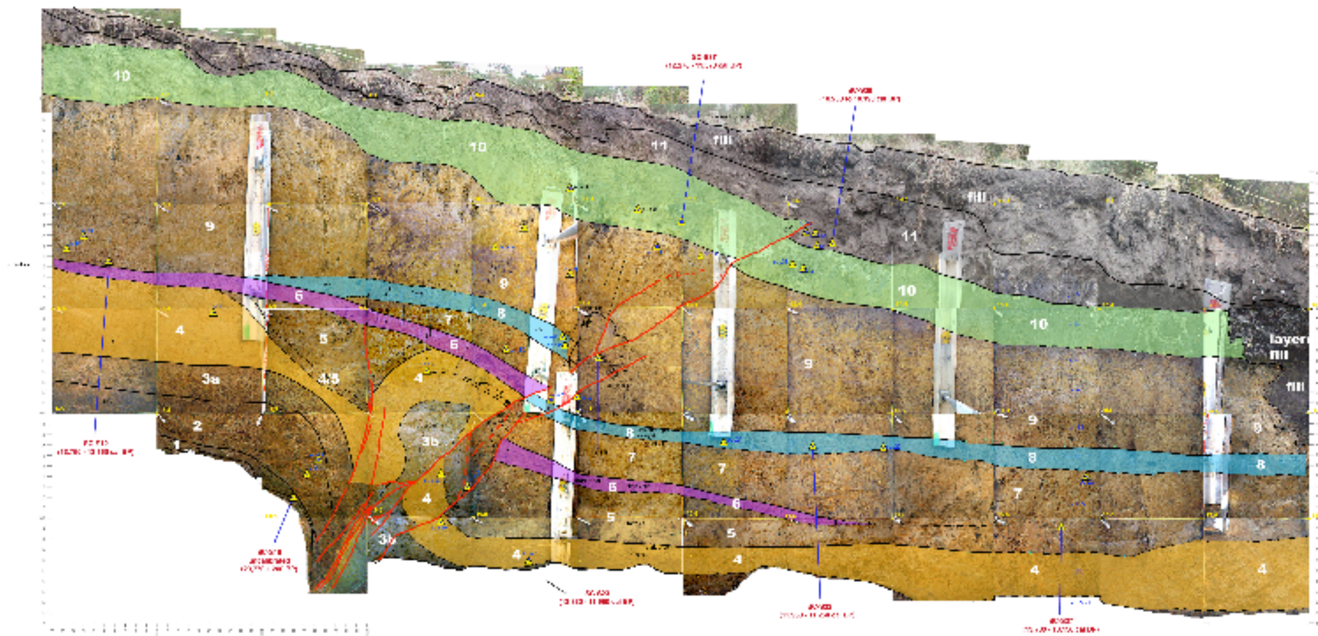

Figure 6 -- Photo mosaic and interpretation of the south wall of the Strong's Creek trench. Highlighted areas represented clayey silt units that are used in the retrodeformation exercise.

using a meshing routine (Figures 7 and 8). This required two assumptions. The first is that the finest-grained units were originally deposited nearly horizontally and not on a pre-existing slope. The second is that surface scarps or warps related to prior deformation events were either removed by erosion or burial. These two assumptions would be confirmed if a) there is relatively little change in lateral thickness of the relatively thin, fine-grained deposits (Figures 7 and 8, Units 4, 6 8 and 10) and b) sedimentary units directly overlying these fine-grained units thicken laterally representing sedimentation across a scarp.

We retrodeformed the north and south wall trench logs from the top (youngest deposits and youngest deformation event) to the bottom. The mesh was deformed in a direction approximately parallel to the dip of the fault. In each retrodeformation step the clayey silt deposits (Figures 7 and 8, Units 4, 6, 8 and 10) were returned to a flat-lying position.

That unit was then removed and underlying units were, in turn, retrodeformed. This allowed us to account for all deformation recorded in the trench in the form of faulting and folding. The oldest, lowest units were progressively deformed during the subsequent events. We recognize that estimates of deformation for these units should include increased error relative to the younger, less deformed deposits. This information allows us to estimate per event fault slip as well as the net offset due to folding (Figures 7 and 8, Table 2).

We identified three distinct deformation events from the trench stratigraphic and structural relations (Figures 7 and 8, Table 2). The amounts of each component of slip were consistent between the two trench walls but varied between the individual events. The net slip (averaged between the two walls) is ~ 4 ± ~1 m, 0.75 ± ~0.2 m and 2 ± ~ 0.5 m for the youngest (Z) to oldest (X) events, respectively. We estimate the amount of net discrete brittle rupture of Unit 10 (Figure 7 and 8) for the most recent event to be about 0.2 m, about 5 % of the total deformation during that event. We can estimate the total net slip based on total deformation of the oldest measurable deposit, Unit 4, through the three events. We estimate an average net slip (from both trench walls) of 5.1 ± 0.4 m. In all but the intermediate event (Y) the horizontal component of slip exceeds the vertical component (Table 2).

We constrain the timing of the deformation events using radiocarbon-based estimates of ages of faulted and unfaulted units. The oldest event, "X" deforms only the deposits as young as Unit 4 (Figures 7 and 8). Sediments deposited subsequent to that unit thicken to the west across the fault reflecting burial of the surface fold. Calibrated ages from samples within Unit 4 range from 13,020 to 13,810 cal BP (SC-N04 and SC-N05, Table 1). A sample collected in the fine sand unit above Unit 4 provides an age of 13,150 to 13,780 cal BP (SC-S27, Table 1). Thus, this event is constrained to have occurred between about 13,000 and 14,000 years BP.

The next deformation event, "Y" involves deposits as young as Unit 8 (Figures 7 and 8). The maximum limiting age for the deposit is 13,150 to 13,780 cal BP (SC-S27, Table 1). Age estimates from samples taken from directly above the unit, range from 11,230 to

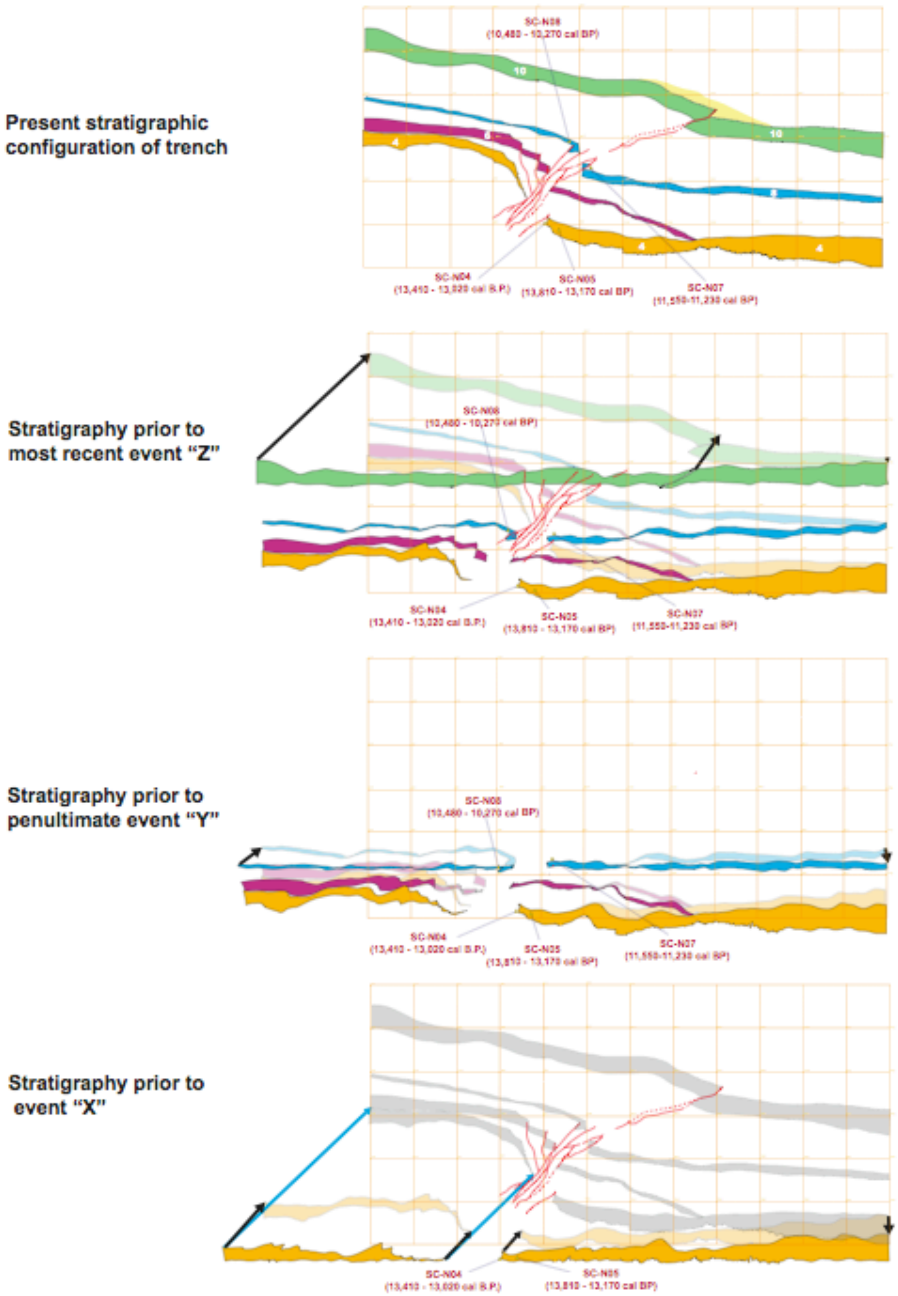

Figure 7 – Retrodeformation of the north wall of the trench. Individual steps in figure represent back step in time of the trench. Faint units represent location of retrodeformed sediments after each faulting event.

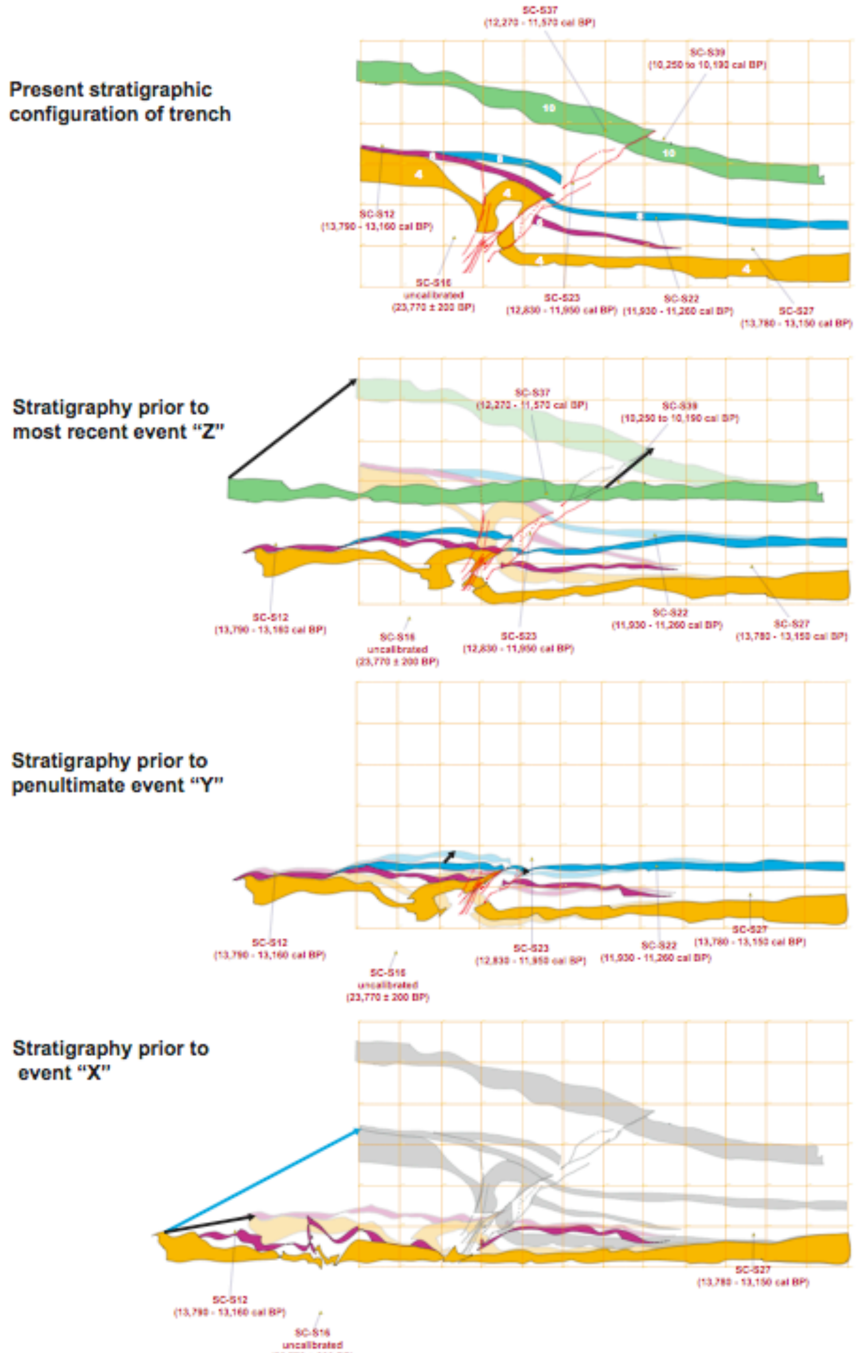

Figure 8 – Retrodeformation of the south wall of the trench. Individual steps in figure represent back step in time of the trench. Faint units represent location of retrodeformed sediments after each faulting event.

11,930 cal BP (SC-N07 and SC-S22, Table 1). Thus the event is constrained between about 11,000 to 13,000 years B.P.

The most recent event is constrained by samples within Unit 10 at 11,570 to 12,270 cal BP (SC-S37, Table 1) and within Unit 11, at 10,190 to 10,250 cal BP (SC-S39) directly above the contact. This constrains the most recent event at between about 10,000 to 12,000 years BP.

Obviously the trench is missing a Holocene section either due to mill-related activity or simply because of change in sedimentation conditions. We still can conclude that this strand of the Little Salmon fault has not experienced a Holocene deformation event unless folding within Unit 10 is due to more than one episode of activity on the fault. The very small amount of discrete rupture of the unit, however, implies that the deformation of this unit is not the product of multiple events.

We calculate a slip rate based on the average total deformation of Unit 4 (Figures 7 and 8, Table 2) of 5.1 m and an age range of 11,000 to 13, 000 years for that event, we can estimate a slip rate of between 0.4 and 0.5 mm/yr.

Table 2 – Components of deformation along the Little Salmon fault at Strong's Creek.

Event	South Wall				North Wall				Average			
	Vertical (m).	Horizontal (m)	Net (m)	Offset (m)	Vertical (m).	Horizontal (m)	Net (m)	Offset (m)	Vertical (m).	Horizontal (m)	Net (m)	Offset (m)
Z	2.5	3.1	4	-	2.4	2.7	3.6	-	2.5	2.9	3.8	-
Event Z (fault only)	0.1	0.2	-	0.2	0.2	0.1	-	0.2	0.1	0.1	-	0.2
Y	0.4	0.2	0.6	-	0.7	0.9	0.9	-	0.55	0.55	0.75	-
X	0.4	2.3	2.3	-	1.0	0.9	1.3	-	0.7	1.6	1.8	-
Total Offset of Unit 4	2.6	4.8	5.5	-	3.3	3.3	4.7	-	3	4.1	5.1	-

It appears that this splay of the fault has had a temporal clustering of events based on the presence of three events in a range of between 1,000 to 4,000 years followed by an absence of activity for the next 10,000 years.

Since other studies provide evidence for substantial Holocene activity on the fault we conclude that there is another splay, likely located beneath the log deck to the east.

REFERENCES

Atwater, B.F., and Hemphill-Haley, E., 1997, Recurrence Intervals for Great Earthquakes of the Past 3,500 Years at Northeastern Willapa Bay, Washington: United States Geological Survey Professional Paper 1576, p. 108.

Carver, G.A., and Burke, R.M., 1988, Trenching investigations of northwestern California faults, Humboldt Bay region, Final report, National Earthquake Hazards Reduction Program,, United States Geological Survey, p. 53.

—, 1992, Late Cenozoic Deformation on the Cascadia Subduction Zone in the Region of the Mendocino Triple Junction, *in* Burke, R.M., and Carver, G.A., eds., Pacific Cell, Friends of the Pleistocene Guidebook for the Field Trip to Northern Coastal California: Arcata, CA, p. 31-63.

Clarke, S.H., Jr., and Carver, G.A., 1992, Late Holocene tectonics and paleoseismicity, southern Cascadia subduction zone: Science, v. 255, p. 188-192.

Goldfinger, C., Nelson, C.H., Johnson, J.E., Erickson, D., Winkler, M., Kalk, P., Pastor, J., Camarero, A., Morri, C., Dunhill, G., Ramos, L., Raab, A., Pisias, N., Jr., Pourmanoutscheri, M., van Rooij, D., Amy, L., and Liu, C.-C.C., 2003, Holocene earthquake records from the Cascadia subduction zone and northern San Andreas Fault based on precise dating of offshore turbidites: Annual Review of Earth and Planetary Sciences, v. 31, p. 555-577.

Kelsey, H.M., 1980, A sediment budget and an analysis of geomorphic process in the Van Duzen River basin, North coastal California, 1941-1975: Geological Society of America Bulletin, v. 91, p. I 190-I 195.

Nelson, A.R., Atwater, B.F., Bobrowsky, P.T., Bradley, L.-A., Clague, J.J., Carver, G.A., Darienzo, M.E., Grant, W.C., Krueger, H.W., Sparks, R.J., Stafford, T.W., and Stuiver, M., 1995, Radiocarbon evidence for extensive plate-boundary rupture about 300 years ago at the Cascadia subduction zone: Nature, v. 378, p. 371-374.

Patton, J.R., 2004, Late Holocene Coseismic Subsidence and Coincident Tsunamis, Southern Cascadia Subduction Zone, Hookton Slough, Wigi (Humboldt Bay), California: Arcata, Humboldt State University.

Tate, A.W., Cashman, S.M., Hemphill-Haley, M.A., Kelsey, H.M., Witter, R.C., and Anonymous, 2005, A deformation analysis of the Little Salmon Fault at Strong's Creek, Humboldt County, California: Abstracts with Programs - Geological Society of America, v. 37, p. 48.

Witter, R.C., Patton, J.R., Carver, G.A., Kelsey, H.M., Garrison-Laney, C., Koehler, R.D., and Hemphill-Haley, E., 2002, Upper Plate Earthquakes on the Western Little Salmon Fault and Contemporaneous Subsidence of Southern Humbodt Bay Over the Past 3,600 Years, Northwestern California: Final Technical Report U.S.

Geological Survey National Earthquake Hazards Reduction Program Award No. 01HQGR0125, p. 44.

Woodward-Clyde Consultants, 1980, Evaluation of the Potential for Resolving the Geologic and Seismic Issues for Humboldt Bay Power Plant Unit No. 3 - Appendixes, prepared for Pacific Gas and Electric Company.